

Robust Compliant Motion for Manipulators, Part II: Design Method

H. KAZEROONI, P. K. HOUPPT, MEMBER, IEEE, AND T. B. SHERIDAN, FELLOW IEEE

Abstract—A controller design methodology to develop a robust compliant motion for robot manipulators is described. The achievement of the target dynamics (the target impedance is introduced in Part I) and preservation of stability robustness in the presence of bounded model uncertainties are the key issues in the design method. State-feedback and force-feedforward gains are chosen to guarantee the achievement of the target dynamics, while preserving stability in the presence of the model uncertainties. In general, the closed-loop behavior of a system cannot be shaped arbitrarily over an arbitrarily wide frequency range. It is proved that a special class of impedances that represent our set of performance specifications are mathematically achievable asymptotically through state-feedback and interaction-force feedforward as actuator bandwidths become large, and we offer a geometrical design method for achieving them in the presence of model uncertainties. The design method reveals a classical trade-off between a system's performance over a bounded frequency range and its stability relative to model uncertainties via multivariable Nyquits criteria. Two classes of such uncertainties are dealt with. While the first class of model uncertainties is formed from the uncertainties in the parameters of the modeled dynamics, the high-frequency unmodeled dynamics form the second class of model uncertainties. The multivariable Nyquist criterion is used to examine trade-offs in stability robustness against approximation of desired target impedances over bounded frequency ranges.

I. INTRODUCTION

THE TARGET DYNAMICS

$$\delta D(s) = (K + Cs + Js^2)\delta Y(s),$$

$$s = j\omega, \delta Y(s) \text{ and } \delta D(s) \in \mathbb{R}^n \quad (1)$$

$$G_i(s) = (K + Cs + Js^2)^{-1}$$

describe the closed-loop behavior for the manipulator. J , C , and K are $n \times n$ real-valued nonsingular matrices selected to parameterize the set of performance specifications (stiffness, ω_0 , and stability given in Part I.) $\delta D(j\omega)$ and $\delta Y(j\omega)$ are $n \times 1$ vectors of deviation of the interaction force¹ and the interaction-port position from equilibrium value in the global cartesian frame. In this paper $(Js^2 + Cs + K)$ is called the *target impedance*.

Although in general the closed-loop behavior of a system

cannot be shaped arbitrarily over an arbitrary frequency range, our goal is to make the manipulator behave according to (1) for all $0 < \omega < \omega_0$. Construction of the eigenstructure of the manipulator according to the eigenstructure of the target dynamics (given in Part I) is the first step in our design method. There are two issues of concern in this step. The first issue addresses the achievement of the eigenstructure of the target dynamics; there is no *a priori* guarantee that the eigenstructure of the manipulator can be constructed according to the eigenstructure of the target dynamics. This limitation in the construction of the eigenstructure is explained in Section III. The second issue concerns the achievement of the target dynamics for some bounded frequency range. Normally, the construction of the eigenstructure of the manipulator according to that of the target dynamics does not guarantee that the closed-loop manipulator behaves dynamically as (1) for all $0 < \omega < \omega_0$. These two issues are answered in Section III. We will prove that the eigenstructure of the target dynamics is achievable. The achievement of the eigenstructure of the target dynamics is made possible by the appropriate choice of the target dynamics. We also prove that the achievement of the eigenstructure of the target dynamics is required to guarantee that the closed-loop system will behave dynamically as (1) for all $0 < \omega < \omega_0$.

If v_i is the right eigenvector of the target dynamics in the joint-angle coordinate frame, then from Part I:

$$v_i = \begin{pmatrix} J_c^{-1} q_i \\ \lambda_i J_c^{-1} q_i \end{pmatrix} \quad (2)$$

where

$$(J\lambda_i^2 + C\lambda_i + K)q_i = 0, \quad q_i \neq 0, \quad i = 1, 2, \dots, 2n. \quad (3)$$

The $2n$ eigenvectors of (2) form a $2n \times 2n$ matrix V :

$$V = (v_1, v_2, \dots, v_{2n}). \quad (4)$$

V is a basis for the state-space representation of the target dynamics in the joint-angle coordinate frame. V shows how the desired modes are coupled among the states of the target dynamics. The $2n$ eigenvalues resulting from (3) are invariant under any linear transformation and form a self-conjugate constant set $\Lambda = \{\lambda_i; i = 1, 2, \dots, 2n\}$. Λ and V taken together describe the eigenstructure of the desired impedance in the joint-angle coordinate frame.

II. DYNAMIC MODEL OF THE MANIPULATORS

We present a dynamic model for a manipulator with actuators suitable for impedance control. We consider two

Manuscript received August 26, 1985; revised February 6, 1986.
H. Kazerooni is with the University of Minnesota, Mechanical Engineering Department, Minneapolis, MN 55455, USA.

P. K. Houpt is with the General Electric, Corporate Research and Development, Schenectady, NY 12345, USA.

T. B. Sheridan is with the Massachusetts Institute of Technology, Mechanical Engineering Department, Cambridge, MA 02139, USA.

IEEE Log Number 8608271.

¹ In this paper *force* implies force and torque and *position* implies position and orientation.

classes of uncertainties in the modeling of the manipulator: the uncertainties in the parameters of the modeled dynamics and high-frequency unmodeled dynamics.

A. Mathematical Modeling

Equation (5) describes the dynamic behavior of the manipulators [8], [9], [19]:

$$M(\theta)\ddot{\theta}(t) + P_g(\theta, \dot{\theta}) + F_g(\theta) = F(t),$$

$$\theta(t), P_g(\theta, \dot{\theta}), F_g(t) \text{ and } F(t) \in \mathbb{R}^n. \quad (5)$$

Vector $F(t) = (f_1(t), \dots, f_n(t))^T$ represents the generalized force. The n -dimensional vectors $P_g(\theta, \dot{\theta})$ and $F_g(\theta)$ are gyroscopic and gravitational forces, respectively. $M(\theta)$ is the symmetric, positive definite, inertia matrix of the manipulator. In most constrained manipulations, the motion of a manipulator is very slow; the system operates at "near stall" conditions, mostly because of dynamic and kinematic constraints. For example, in grinding and metal cutting, the state of the art in current technology is the limiting factor in the speed of such operations. The orders of magnitude of the gyroscopic terms are much smaller than the inertia and the gravity terms in constrained maneuvers; this suggests the elimination of the gyroscopic terms from the differential equations of the motion. This elimination is mathematically equivalent to the linearization of the gyroscopic terms in the neighborhood of an equilibrium point (zero velocity). This point is characterized by the vector θ_0 . At this stage, the assumption that the manipulator moves slowly does not imply any specific restraint on the inputs to (5). In general, there is no unique characterization associated with the inputs that can generate large-velocity terms. The above assumption rejects all inputs that could give rise to velocity terms. We will clarify the conditions on the inputs that will guarantee small velocities. At this stage, it is sufficient to assume that all velocity terms are close to zero. This automatically ensures that the inputs to (5) will satisfy the conditions. $F_g(\theta_0) = F_0$ is true at equilibrium. If $\delta\theta(t)$ is the perturbation of the generalized coordinate from θ_0 and $\delta F(t)$ is the perturbation of the generalized force from F_0 , then the linearized equation of motion is

$$M(\theta_0)\delta\ddot{\theta}(t) + GR(\theta_0)\delta\dot{\theta}(t) = \delta F(t),$$

$$\delta F(t) \text{ and } \delta\theta(t) \in \mathbb{R}^n \quad (6)$$

where $GR(\theta_0)$ is an $n \times n$ matrix that can be computed from the following equation:

$$GR(\theta_0) = \begin{pmatrix} \frac{\partial F_g(\theta)}{\partial \theta_1(t)} & \frac{\partial F_g(\theta)}{\partial \theta_2(t)} & \dots & \frac{\partial F_g(\theta)}{\partial \theta_n(t)} \end{pmatrix} \quad \text{for } \theta = \theta_0. \quad (7)$$

Since the velocity terms in $P_g(\theta, \dot{\theta})$ are of the form $\dot{\theta}_i(t)^2$ or $\dot{\theta}_i(t)\dot{\theta}_j(t)$, the linearized form of the gyroscopic terms around the equilibrium point $\theta_0(t)$ vanish from the linearized equations. Note that the target dynamics are also expressed at equilibrium point. $M(\theta_0)$ and $GR(\theta_0)$ are functions of the configuration of the system, and they change once the

manipulator moves from one point to another point. We plan to update $M(\theta_0)$ and $GR(\theta_0)$ as θ_0 changes. Equation (6) represents the dynamic behavior of a manipulator when its motion is slow. Gravity and the inertia of the system are two effects that practitioners always observe in the behavior of the manipulators at low speeds; gravity dominates the motion of the system at very low frequencies, while inertia affects the behavior of the system in the higher frequency range. The generalized force $\delta F(t)$ can be expressed by

$$\delta F(t) = T_s \delta T(t) + J_c^T \delta D(t) \quad (8)$$

where $\delta T(t) = (\delta t_1(t), \dots, \delta t_n(t))^T$ and $\delta D(t) = (\delta d_1(t), \dots, \delta d_n(t))^T$ are the perturbation of the interaction force in the global coordinate frame and the perturbation of the actuator torques, respectively. T_s is a nonsingular square matrix which represents the effect of $\delta T(t)$ on the coordinates. If the coordinates are independently driven by actuators, then $T_s = I_{nn}$. An example of a nonunity T_s arises when $\delta\theta(t)$ is measured absolutely while some actuators are not driving the joint angles from a stationary base. Substituting (8) in (6) yields (9) for the linearized dynamics of the manipulators:

$$M(\theta_0)\delta\ddot{\theta}(t) + GR(\theta_0)\delta\dot{\theta}(t) = T_s \delta T(t) + J_c^T \delta D(t) \quad (9)$$

where $\delta\theta(t) = (\delta\theta_1(t), \dots, \delta\theta_n(t))^T$ expresses the perturbed joint-angles. Equation (10) approximates the dynamic behavior of each actuator. Thus

$$\frac{\delta \dot{t}_i(t)}{\lambda_{ai}} + \delta t_i(t) = \delta u_i(t), \quad i = 1, 2, \dots, n. \quad (10)$$

$\delta u_i(t)$ and $\delta t_i(t)$ are input force and output-torque perturbation for each actuator, respectively. λ_{ai} is the bandwidth of each actuator. Equation (10) is scaled to produce one unit of torque for each unit of input at equilibrium. Such scaling is common and can always be compensated for at the end of the design procedure by adjusting the open-loop transfer function matrix. Note that (10) is only an approximation of the dynamics of an actuator, which has been widely used by practitioners (20). One may equally choose higher order dynamics for actuators which will cause A_a to be of higher dimensions. The set of differential equations describing the actuation of the manipulator is approximated by

$$\delta \dot{T}(t) = A_a \delta T(t) + B_a \delta U(t) \quad (11)$$

where

$$A_a = \text{diag} (-\lambda_{a1}, -\lambda_{a2}, \dots, -\lambda_{an})$$

$$B_a = \text{diag} (\lambda_{a1}, \lambda_{a2}, \dots, \lambda_{an})$$

$$\delta U(t) = (\delta u_1(t), \delta u_2(t), \dots, \delta u_n(t))^T$$

$$\delta T(t) = (\delta t_1(t), \delta t_2(t), \dots, \delta t_n(t))^T.$$

Combining (9) and (11) yields (12) for the dynamics of the

manipulator and the actuators:

$$\begin{pmatrix} \delta\dot{\theta}(t) \\ \delta\ddot{\theta}(t) \\ \delta\dot{T}(t) \end{pmatrix} = \underbrace{\begin{pmatrix} 0_{nn} & I_{nn} & 0_{nn} \\ -M^{-1}(\theta_0)GR(\theta_0) & 0_{nn} & M^{-1}(\theta)T_s \\ 0_{nn} & 0_{nn} & A_a \end{pmatrix}}_A \begin{pmatrix} \delta\theta(t) \\ \delta\dot{\theta}(t) \\ \delta T(t) \end{pmatrix} \\ \delta\dot{X}(t) \qquad \qquad \qquad \delta X(t) \\ + \underbrace{\begin{pmatrix} 0_{nn} \\ 0_{nn} \\ B_a \end{pmatrix}}_B \delta U(t) + \underbrace{\begin{pmatrix} 0_{nn} \\ M^{-1}(\theta_0)J_c^T \\ 0_{nn} \end{pmatrix}}_L \delta D(t). \quad (12)$$

If $H = (I_{nn} \ 0_{nn} \ 0_{nn})$, then

$$\delta\dot{X}(t) = A\delta X(t) + B\delta U(t) + L\delta D(t) \quad (13)$$

$$\delta\theta(t) = H\delta X(t) \quad (14)$$

where $\delta X(t) \in \mathbb{R}^{3n}$; $\delta U(t)$, $\delta D(t)$ and $\delta\theta(t) \in \mathbb{R}^n$; (A, B) is a controllable pair; and (A, H) is an observable pair.

Generally speaking, if the bandwidths of the actuators are much greater than ω_0 in all directions, then the actuator dynamics can be neglected in dynamic equation (12). Neglecting all actuator dynamics results in $2n$ -state differential equations for the manipulator. Conversely, if an actuator bandwidth is smaller than ω_0 in a given direction, then the actuator dynamics cannot be neglected. Matrix A has $2n$ eigenvalues associated with the manipulator dynamics and n eigenvalues describing the actuator's bandwidth. If the transfer function matrix that maps $\delta U(j\omega)$ to $\delta\theta(j\omega)$ is $G_p(j\omega)$, then $\delta\theta(j\omega) = G_p(j\omega)\delta U(j\omega)$, where

$$G_p(j\omega) = H(j\omega I_{3n} - A)^{-1}B. \quad (15)$$

The mathematical model given by (12) is a fair approximation of the nonlinear dynamics represented by (5) as long as $\delta U(t)$ and $\delta D(t)$ are bounded in *magnitude* and *frequency*. Equation (12) is the linearized version of a set of nonlinear differential equations in the neighborhood of an arbitrary zero-velocity operating point. The model is therefore valid as long as the velocity terms are close to zero. The smaller the magnitude of the inputs, the closer the model will be to reality because small inputs result in small velocities as long as the frequency range of operation of the inputs is bounded. Note that by confining the frequency range of $\delta D(t)$ and $\delta U(t)$ to all $0 < \omega < \omega_0$ and the magnitudes of $\delta U(t)$ and $\delta D(t)$ to very small values, a designer can eliminate all inputs that could give rise to significant joint-angle velocities.

B. Model Uncertainties

Even though some mathematical models reliably represent the dynamics of a manipulator, no nominal model can imitate a manipulator completely. No mathematical model is more than an approximation of reality; none is absolutely true. The mathematical model given by (12) will yield a rational approximation of the dynamics of manipulators for a certain range of inputs ($\delta U(t)$ and $\delta D(t)$), which is bounded in *magnitude* and *frequency*. Outside this range, the model will

depart from reality. The difference in behavior between the model and the real system in various operating regions must be taken into account through a meaningful mathematical method that allows for differences between ideal and real systems. Such discrepancies are called model uncertainties. Let $G'_p(j\omega)$ represent the true dynamics of the manipulator. Satisfying the condition on the input magnitudes, (16) can be written to show the relationship between the nominal model $G_p(j\omega)$ and the true dynamics $G'_p(j\omega)$ by means of $E(j\omega)$ [14], [1]. Thus²

$$G'_p(j\omega) = G_p(j\omega)(I_{nn} + E(j\omega)) \quad (16)$$

$$\sigma_{\max}(E(j\omega)) < e(\omega), \quad \text{for all } \omega \geq 0. \quad (17)$$

$E(j\omega)$ is called the unstructured model uncertainty because (16) does not imply any mechanism or structure that gives rise to $E(j\omega)$. $e(\omega)$ is a positive scalar function, which confines $G'_p(j\omega)$ to a neighborhood of $G_p(j\omega)$ with magnitude $e(\omega)$. We assume that $G'_p(j\omega)$ in (16) remains a strictly proper, finite system. We also assume that $G'_p(j\omega)$ has the same number of unstable modes as $G_p(j\omega)$. The unstable modes of $G_p(j\omega)$ and $G'_p(j\omega)$ need not be identical. Therefore, $E(j\omega)$ may be an unstable operator. When (16) is used to represent various unmodeled dynamics of manipulators, the limiting function $e(\omega)$ has the form shown in Fig. 1. $e(\omega)$ is a bound for unstructured uncertainties. It is nonzero for all frequencies.

$e(\omega)$ is usually smaller than unity at low frequencies and increases to unity and above at high frequencies. High-frequency dynamics caused by time delays, electrical resonances, structure dynamics, etc., always exist but are neglected. This causes (12) to significantly contradict reality at high frequencies.

Lack of knowledge about the precise inertia matrix, the size of the inputs, the effects of perturbations from operating points, nonlinearities such as saturation, etc., give rise to an $e(\omega)$ at all frequencies, while high-frequency unmodeled dynamics contribute significantly to the magnitude of $e(\omega)$ at high frequencies. Saturation is inherently nonlinear but can be modeled as open-loop gain reduction for all frequencies. Since $e(\omega)$ assumes a single worst-case magnitude applicable in all directions, it is helpful to determine the slowest unmodeled mode in the manipulator. Let the frequency range associated with this mode be ω_v . A good estimation of ω_v allows the designer to determine the frequency range for which the model is nearly valid. (No model is absolutely valid.) This estimation is necessary because it is meaningless to consider (1) as an expression of the target dynamics for all $0 < \omega < \omega_0$ when the frequency range for which the model can be trusted is unknown. Models must be nearly valid for the entire frequency range through which the target dynamics are expected to occur, i.e., $\omega_0 < \omega_v$. Fig. 1 shows the relative sizes of ω_v and ω_0 . The upper bound for ω_0 can be selected from equation $\omega_v = c\omega_0$ where c is a constant number whose size depends on

² The maximum singular value of $E(j\omega)$ is defined as

$$\sigma_{\max}[E(j\omega)] = \max \frac{\|E(j\omega)x\|}{\|x\|}$$

where $x \neq 0$, and $\|\cdot\|$ denotes the Euclidean norm (4).

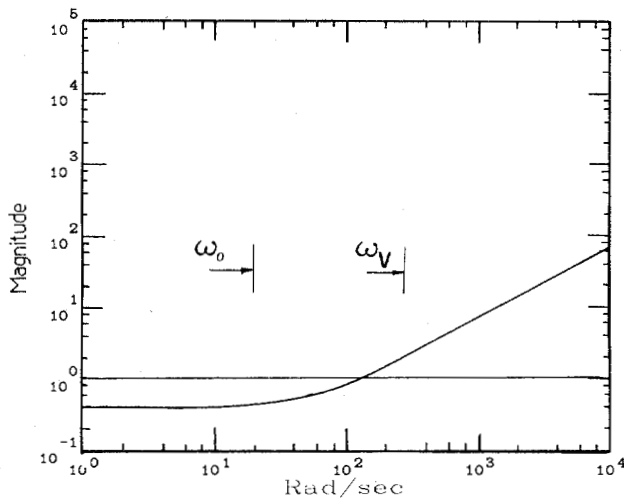


Fig. 1. $e(\omega)$ is a conservative and educated guess about the difference in model of the system and the real system.

the damping of the unmodeled mode. A well-damped unmodeled mode requires a small c (perhaps somewhere between five and ten), while an underdamped mode requires a large c (could be as large as 100). The value of ω_v and a conservative guess for c assign an upper bound for ω_0 . To meet stability robustness specifications, it is necessary to have a conservative guess for $e(\omega)$ for all $0 < \omega < \infty$. This is because our stability robustness test is a sufficient condition which must be satisfied for all $0 < \omega < \infty$ [14]. Experience, a good understanding of the system, and high-performance experimental equipment will enable a designer to make a good guess as to the magnitude of $e(\omega)$ for a wide frequency range. $e(\omega)$ is an educated guess about the difference between the model of the system and the real system, which must be supplied by the designer. Here we assume that a conservative guess for $e(\omega)$ is given, along with (12), to represent the model uncertainty in the system. To recapitulate, the model in (12) is considered nearly valid as long as the following conditions are satisfied.

1) $\delta D(t)$ and $\delta U(t)$ must contain components whose frequency spectra are less than ω_0 . ω_0 must be selected so that $\omega_0 < \omega_v$. This is because of the significant difference between the model and the reality of the system for $\omega_v < \omega < \infty$.

2) $\delta D(t)$ and $\delta U(t)$ must be small enough in magnitude to meet the linearization conditions. (In theory, $\delta D(t)$ and $\delta U(t)$ must approach zero.)

III. COMPENSATOR DESIGN

This section presents a controller design technique that guarantees manipulators represented by dynamic (12) will behave dynamically like (1) for all $0 < \omega < \omega_0$. Since we plan to shape a frequency-domain relationship between $\delta D(j\omega)$ and $\delta Y(j\omega)$, we must not consider the dependence of $\delta D(t)$ on the dynamics of the environment in this analysis. This allows us to preserve $\delta D(j\omega)$ so we can arrive at a relationship between $\delta D(j\omega)$ and $\delta Y(j\omega)$. It is assumed that all states $\delta X(t)$ and interaction forces $\delta D(t)$ in (12) can be measured. The states of the system are joint-angles, joint-angle rates, and actuator torques. There are no acceleration measurements. Suppose the

control law in (13) is chosen so that

$$\delta U(t) = -G\delta X(t) + G_d\delta D(t) \quad (18)$$

where $G = n \times 3n$, and $G_d = n \times n$. Substituting $\delta U(t)$ in (13) yields

$$\delta \dot{X}(t) = (A - BG)\delta X(t) + (L + BG_d)\delta D(t) \quad (19)$$

$$\theta(t) = H\delta X(t) \quad (20)$$

Fig. 2 shows the closed-loop system. G_d can be considered a feedforward gain and not feedback gain. This is true in our treatment of force measurement, and G_d does not affect the stability of the closed-loop system. Even though $\delta D(t)$ can be expressed as a function of the dynamics of the environment, in this section we must ignore this dependence so we can arrive at a relationship between $\delta Y(j\omega)$ and $\delta D(j\omega)$ in the frequency domain. The state-feedback gain G and the force-feedforward gain G_d are designed to guarantee that the three transformation matrices $(A - BG)$, $(L + BG_d)$, and H in (19) and (20) result in the same transfer-function matrix in the global coordinate frame as the target impedance, which is expressed in (1). In other words, if $G_{cl}(j\omega)$ represents a mapping from the interaction force $\delta D(j\omega)$ to the joint angles $\delta\theta(j\omega)$, then the objective is to design G and G_d so that (21) is satisfied for all $0 < \omega < \omega_0$, while the stability robustness specifications are also guaranteed. $\delta D(j\omega)$ is measured in the global coordinate frame, so

$$J_c G_{cl}(j\omega) = G_t(j\omega) \quad (21)$$

where

$$G_{cl}(j\omega) = H(j\omega I_{3n} - A + BG)^{-1}(L + BG_d)$$

$$\delta\theta(j\omega) = G_{cl}(j\omega)\delta D(j\omega).$$

$J_c G_{cl}(j\omega)$ represents the transfer-function matrix that maps the interaction force $\delta D(j\omega)$, to the end-point position $\delta Y(j\omega)$ in the global coordinate frame.

A. State-Feedback Design

G is designed to guarantee the *eigenstructure* represented by V and Λ and the *stability robustness specification*. The complex number s_i and the complex vector u_i which satisfy (22), are the closed-loop eigenvalue and the right closed-loop eigenvector of (19). Thus

$$s_i u_i = (A - BG)u_i, \quad u_i \neq 0_{3n}, \quad i = 1, 2, \dots, 3n \quad (22)$$

where u_i is a $3n \times 1$ vector. For convenience, matrix U is formed such that it contains all right closed-loop eigenvectors u_i as its columns, and a self-conjugate set S is formed such that it contains all closed-loop eigenvalues as its members:

$$U = (u_1, u_2, \dots, u_{3n}) \quad (23)$$

$$S = \{s_i : i = 1, 2, \dots, 3n\}. \quad (24)$$

The objective is to design G so that $(A - BG)$ contains the eigenstructure represented by Λ and V . Aside from the case of a single input system, the specification of closed-loop eigen-

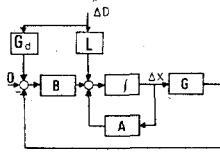


Fig. 2. Closed-loop system.

values does not uniquely define G . The source of nonuniqueness is the freedom offered by state feedback, beyond eigenvalue assignment, in selecting the associated right closed-loop eigenvectors (or left closed-loop eigenvectors) and generalized eigenvectors from an allowable sub-space. Arbitrary eigenvector assignment in general is not possible. Each closed-loop eigenvector is confined to an allowable sub-space. This allowable sub-space is given in Sections III-A-1 and 2. The restriction on the construction of the closed-loop eigenvectors simply implies that one cannot specify all members of each right eigenvector arbitrarily. Only some partitions of each eigenvector in general can be constructed according to design specifications. A unique value for G is determined by the arbitrary pole-placement of S and by the eigenvector construction of U in the allowable subspace [2], [3], [12], [15]–[17]. In other words, a unique value of G can be designed so that the following holds:

- the $2n$ dominant closed-loop eigenvalues in S are placed at locations assigned by Λ . The n remaining actuator eigenvalues are moved as far to the left as the stability robustness specifications will allow (see Section III-C).
- U is constructed in the allowable sub-space so that the dominant partition of U contains V .

Since u_i and v_i belong to different spaces, it is necessary to partition U . Here we describe the dominant partition of U and explain how U can be constructed such that it contains V . Partitioning U yields

$$U = \begin{pmatrix} U_{11} & U_{12} \\ U_{21} & U_{22} \end{pmatrix} \quad (25)$$

where $U_{11} = 2n \times 2n$, $U_{12} = 2n \times n$, $U_{21} = n \times 2n$, and $U_{22} = n \times n$. Assume also that $U = (U_1 \ U_2)$, where

$$U_1 = \begin{pmatrix} U_{11} \\ U_{21} \end{pmatrix}, \quad U_2 = \begin{pmatrix} U_{12} \\ U_{22} \end{pmatrix}.$$

U_1 is the set of right closed-loop eigenvectors associated with the $2n$ dominant closed-loop eigenvalues represented by Λ . U_2 is the set of right closed-loop eigenvectors associated with the n actuator closed-loop eigenvalues. U_{11} shows the contribution of the $2n$ dominant closed-loop eigenvalues to the manipulator states $(\delta\theta(t), \delta\dot{\theta}(t))$, while U_{21} shows the effect of the $2n$ dominant eigenvalues on the actuator states $\delta T(t)$. We construct U_1 such that $U_{11} = V$. In general, because of limitations on eigenstructure construction, a designer cannot form the closed-loop eigenvectors arbitrarily. But in this case, it is possible to construct U_1 so that $U_{11} = V$. In other words V , which is the set of right eigenvectors of the target dynamics of (1), is in the allowable subspace determined by the open-loop dynamics. The existence of the right eigenvectors of the

target impedance in the allowable subspace determined by the open-loop dynamics given by (13) is a significant factor in achieving the target impedance. If V were not in the allowable sub-space, the achievement of V and Λ , and consequently the target dynamics of (1) would not be possible by state-feedback design. This allowable subspace is given in the sections to follow. Once U_{11} is constructed to be exactly like V , no choice will remain in constructing U_{21} .

U_{12} shows the effect of nondominant closed-loop eigenvalues on the manipulator states. U_{22} is the more significant partition of U_2 because it allows the achievement of the uncoupled closed-loop dynamics for the actuators. Once U_{22} is constructed to achieve the uncoupled closed-loop behavior for the actuators, no choice will remain in the construction of U_{12} . This issue is explained in Section III-A-2. Because of the mentioned limitation on the construction of the eigenvectors, only some partitions of the eigenvectors can be constructed arbitrarily. Designers must construct those partitions of eigenvectors that have a more significant role in the closed-loop behavior. In our case, U_{11} and U_{22} are more significant partitions of U_1 and U_2 , respectively. The exact construction of U_{11} and U_{22} and the placement of the $3n$ poles of S are the free choices that linear state-feedback control offers for achieving a unique gain, G . Sections III-A-1 and III-A-2 explain how this freedom can be used.

1) *Manipulator Eigenstructure*: This section identifies how the manipulator eigenstructure can be constructed. Using (22), (26) can be written to express the right closed-loop eigenvector u_i associated with the $2n$ dominant eigenvalues. From (22)

$$(s_i I_{3n3n} - A)u_i + BGu_i = 0_{3n}, \quad u_i \neq 0_{3n}, \quad i = 1, 2, \dots, 2n. \quad (26)$$

Since s_i is selected from set Λ , then $s_i = \lambda_i$. Equation (26) can also be written as:

$$((\lambda_i I_{3n3n} - A) - B) \begin{pmatrix} u_i \\ m_i \end{pmatrix} = 0_{3n}, \quad i = 1, 2, \dots, 2n \quad (27)$$

where $m_i = -Gu_i$. Equation (27) states that $(u_i^T \ m_i^T)^T$ is in the right null-space of $[(\lambda_i I_{3n3n} - A) - B]$. Since the dimension of the right null-space of $[(\lambda_i I_{3n3n} - A) - B]$ is at least n [20], $(u_i^T \ m_i^T)^T$ is confined in an n -dimensional subspace spanned by null vectors of $[(\lambda_i I_{3n3n} - A) - B]$. Because of this restriction on $(u_i^T \ m_i^T)^T$, not all members of u_i can be selected arbitrarily. u_i must be selected such that $(u_i^T \ m_i^T)^T$ lies in the null-space of $[(\lambda_i I_{3n3n} - A) - B]$. There is another way of arriving at this confinement. If s_i does not belong to the spectrum of A , then (28) can be generated from (22):

$$u_i = -(s_i I_{3n3n} - A)^{-1} BGu_i, \quad i = 1, 2, \dots, 2n. \quad (28)$$

Since s_i is selected from set Λ , then $s_i = \lambda_i$. u_i can also be expressed by (29). Thus

$$u_i = (\lambda_i I_{3n3n} - A)^{-1} Bm_i, \quad i = 1, 2, \dots, 2n \quad (29)$$

$$m_i = -Gu_i, \quad (30)$$

where m_i is an $n \times 1$ vector. Equation (29) mathematically justifies the limitation on the construction of the closed-loop eigenvector mentioned previously [7]. Each closed-loop eigenvector u_i associated with λ_i must reside in the column space of $(\lambda_i I_{3n3n} - A)^{-1}B$, which is a function of the closed-loop eigenvalue λ_i and the open-loop dynamics of the manipulator (A, B) . This is an important constraint on the construction of the right closed-loop eigenvector u_i , which is trapped in the n -dimensional subspace established by columns of $(\lambda_i I_{3n3n} - A)^{-1}B$. Because of the confinement of u_i in an n -dimensional subspace, in general, it can be expected that only n members of u_i can be selected arbitrarily. But we are interested in construction of u_i such that its first $2n$ members are like v_i . We show that a vector u_i , (along with an m_i) exists such that $(u_i^T \ m_i^T)^T$ is in the null-space of $[(\lambda_i I_{3n3n} - A) - B]$ and its first $2n$ members are the same as v_i . Consider u_i and m_i given by

$$u_i = \begin{pmatrix} I_{nn} \\ \lambda_i I_{nn} \\ T_s^{-1}[M(\theta_0)\lambda_i^2 + GR(\theta_0)] \end{pmatrix} J_c^{-1} q_i, \quad i = 1, 2, \dots, 2n \quad (31)$$

and

$$m_i = B_a^{-1}(\lambda_i I_{nn} - A_a) T_s^{-1}[M(\theta_0)\lambda_i^2 + GR(\theta_0)] J_c^{-1} q_i, \quad i = 1, 2, \dots, 2n. \quad (32)$$

The first $2n$ members of u_i are the same as v_i . From $[(s_i I_{3n3n} - A) - B]$:

$$[(s_i I_{3n3n} - A) - B] = \begin{pmatrix} s_i I_{nn} & -I_{nn} & 0_{nn} & 0_{nn} \\ M^{-1}(\theta_0)GR(\theta_0) & s_i I_{nn} & -M^{-1}(\theta_0)T_s & 0_{nn} \\ 0_{nn} & 0_{nn} & s_i I_{nn} - A_a & -B_a \end{pmatrix}. \quad (33)$$

Substituting for $[(s_i I_{3n3n} - A) - B]$ from (33) when $S_i = \lambda_i$, and u_i and m_i from equations (31) and (32) into (27), shows that $(u_i^T \ m_i^T)^T$ is in the null space of $[(\lambda_i I_{3n3n} - A) - B]$. In fact, we arrived at (31) and (32) by obtaining the right null-space of $[(s_i I_{3n3n} - A) - B]$. This substitution shows that u_i , which is given by (31), is achievable. Since $u_i (i = 1, 2, \dots, 2n)$ must be in the right null space of $[(\lambda_i I_{3n3n} - A) - B]$, then no option would remain in constructing the last n members of u_i if the first $2n$ members of u_i are constructed like v_i .

2) *Actuator Eigenstructure*: We offer a similar treatment for the actuator eigenvalues and their corresponding right eigenvectors. The actuators in the manipulators are dynamically uncoupled. It is a good practice to preserve this uncoupling in the dynamics of the actuators in the closed-loop case, too. The uncoupling of the closed-loop actuator dynamics allows the designers to achieve different bandwidths for actuators such that they are consistent with their hardware.

It has already been mentioned that U_{22} is the significant partition of U_2 . To achieve the uncoupling of the actuators, U_{22} is chosen to be an identity matrix. Since each right closed-loop eigenvector is confined to an n -dimensional subspace in $3n$ -dimensional space, constructing U_2 such that $U_{22} = I_{nn}$ is always possible. At this stage, we have not mentioned where the n actuator closed-loop eigenvalues must be located. This will depend on the stability robustness specifications. Section III-C is devoted to this matter. For continuity in all material concerning the design of G , readers can assume that the closed-loop eigenvalues of the actuators are located deeper in the left complex plane than any complex number offered by Λ . At this point, it does not matter how far from the origin these eigenvalues are located. Section III-C clarifies how a designer can use the freedom of choosing the closed-loop eigenvalues of the actuators to satisfy the robustness specifications. If $m_i = -Gu_i$, (22) can be written as

$$[(s_i I_{3n3n} - A) - B] \begin{pmatrix} u_i \\ m_i \end{pmatrix} = 0_{3n}, \quad i = 2n+1, 2n+2, \dots, 3n. \quad (34)$$

Let

$$U_{22} = (g_1, g_2, \dots, g_n) \quad (35)$$

where g_i is a $n \times 1$ vector and $U_{22} = I_{nn}$. If u_i and m_i are selected according to (36) and (37)

$$U_i = \begin{pmatrix} [M(\theta_0)s_i^2 + GR(\theta_0)]^{-1}T_s \\ [M(\theta_0)s_i^2 + GR(\theta_0)]^{-1}T_s s_i \\ I_{nn} \end{pmatrix} g_i, \quad i = 2n+1, 2n+2, \dots, 3n \quad (36)$$

$$m_i = B_a^{-1}(s_i I_{nn} - A_a) g_i, \quad i = 2n+1, 2n+2, \dots, 3n \quad (37)$$

then substituting u_i and m_i from (36) and (37) into (34) and $[(s_i I_{3n3n} - A) - B]$ from (33) into (34) shows that $(u_i^T \ m_i^T)^T$ is in the right null-space of $[(s_i I_{3n3n} - A) - B]$. This shows that u_i , which is given by (36), is achievable. The last n members of u_i are like g_i , which guarantees the uncoupling of the closed-loop actuator dynamics. Note that the inverse of $[M(\theta_0)s_i^2 + GR(\theta_0)]$ always exists as long as s_i is not equal to any eigenvalues of A . One can always multiply u_i by $[M(\theta_0)s_i^2 + GR(\theta_0)]$ to ease this condition. Since $u_i (i = 2n+1, 2n+2, \dots, 3n)$ must be in the right null space of $[(s_i I_{3n3n} - A) - B]$, no option would remain in constructing the first $2n$ members of u_i , if the last n members of u_i are constructed like v_i .

3) *Computation of G* : Once the m_i and u_i are computed from (31), (32), (36), and (37), then (30) can be used to derive

$$G = -[m_1, m_2, \dots, m_{3n}][u_1, u_2, \dots, u_{3n}]^{-1} \quad (38)$$

or equivalently

$$G = -[m_1, m_2, \dots, m_{3n}]U^{-1} \quad (39)$$

for G . Equation (39) requires that U , given by (25), is a full matrix. Since the target dynamics are simple³ [5], [13], [10], then U_{11} , which is equal to V , is a full rank matrix. This means that U_1 is a $2n$ -rank matrix. Matrix U_2 must be constructed such that $(U_1 \ U_2)$ is a full-rank matrix.

However, since there is freedom in the selection of the eigenvalues and eigenvectors of the actuators, one can always use this freedom to modify U_2 such that $(U_1 \ U_2)$ is a full-rank matrix. We do not give a general procedure to construct U_2 such that $(U_1 \ U_2)$ is a full-rank matrix. Here we prove that if all closed-loop eigenvalues of the actuators approach infinity at any angle in the left half complex plane, then U is a full rank matrix. It can be verified that as actuator eigenvalues approach negative large numbers, each of the upper $2n$ members of each right eigenvector in (36) approaches a small number, while the last n members stay constant. This implies that the members of U_{12} of matrix U in (25) will be much smaller than U_{22} . Suppose $(U_1 \ U_2)$ is not a full-rank matrix, then there exists at least one column in U_2 , which belongs to the column space of U_1 (U_1 is a full-rank matrix) as eigenvalues of the actuators approach infinity at any angles in the left half complex plane. Since, in the limit, all members of U_{12} are almost zero, this leads to the dependence of the columns of U_{11} . This is a contradiction because U_{11} is a full-rank matrix. The above discussion only guarantees the existence of U^{-1} when all the eigenvalues of the actuators approach infinity in a stable sense. In practice, we plan to locate the actuator eigenvalues deeper in the left-half complex plane than any complex number offered by Λ . If U is a full-rank matrix, then U^{-1} can be computed as

$$\begin{pmatrix} [U_{11} - U_{12}U_{22}^{-1}U_{21}]^{-1} \\ -U_{22}^{-1}U_{21}[U_{11} - U_{12}U_{22}^{-1}U_{21}]^{-1} \end{pmatrix}$$

Note that we do not consider the independence of the columns of U as a condition for the achievability of the target impedance. This is because one can always use the freedom in choosing the eigenvalues of the actuators to construct U_2 such that $(U_1 \ U_2)$ is full rank as long as U_1 is a full-rank matrix, which will be true if the target impedance is simple. Since U and S are self-conjugate, then G will always be a real matrix (15). Knowing the requirements for the independence of the right eigenvectors of the target dynamics, we can write explicitly the only set of formal conditions that guarantees the structure of the target dynamics will be mathematically achievable: J , C , and K must be nonsingular, and the target dynamics must be simple (V must be a full rank matrix.)

B. Force-Feedforward Design

The previous section provides a method for designing the state-feedback gain G to guarantee the eigenstructure of the target dynamics given by Λ and V . Assuring that the eigenstructure of the target dynamics is achievable does not imply that the target dynamics given by (1) can be achieved. The following theorem formally states the conditions under

which a designer can guarantee that the system will follow the target dynamics, given by (1), governing the closed-loop behavior of the manipulators for all $0 < \omega < \omega_b$. $(0, \omega_b)$ is the bounded frequency range in which the system may operate.

1) *Theorem*: The state-space representation of the dynamic system given by (12), with state-feedback gain G and force-feedforward gain G_d , is given by

$$\delta \dot{X}(t) = (A - BG)\delta X(t) + (L + BG_d)\delta D(t),$$

$$G = n \times 3n, \quad G_d = n \times n \quad (41)$$

$$\delta \theta(t) = H\delta X(t) \quad (42)$$

where $\delta \theta(t)$ and $\delta D(t) \in \mathbb{R}^n$. The closed-loop transfer-function matrix that maps $\delta D(j\omega)$ to $\delta \theta(j\omega)$ is given by

$$G_{cl}(j\omega) = H(j\omega I_{3n} - A + BG)^{-1}(L + BG_d) \quad (43)$$

where $\delta \theta(j\omega) = G_{cl}(j\omega)\delta D(j\omega)$. Suppose all actuator closed-loop eigenvalues are selected to satisfy the inequality

$$|s_i| > \rho, \quad \text{real}(s_i) < 0, \quad i = 2n+1, 2n+2, \dots, 3n \quad (44)$$

where ρ is a positive scalar. If ρ approaches ∞ , and if G is designed according to Section III-A to guarantee the target eigenstructure V and Λ for the closed-loop system, then a unique value for G_d can be obtained such that limit (45) is true

$$\lim_{\rho \rightarrow \infty} \begin{pmatrix} -U_{11}^{-1}U_{12}[U_{22} - U_{21}U_{11}^{-1}U_{12}]^{-1} \\ [U_{22} - U_{21}U_{11}^{-1}U_{12}]^{-1} \end{pmatrix} \quad (40)$$

for all ω in the bounded interval $(0, \omega_b)$. Thus

$$\lim_{\rho \rightarrow \infty} J_c G_{cl}(j\omega) = G_r(j\omega). \quad (45)$$

This theorem does not prescribe any value for G_d . It justifies the conditions under which limit (45) is true for all $0 < \omega < \omega_b$ without regard to stability robustness. According to this theorem the satisfaction of inequality 44 when ρ approaches ∞ and the selection of G such that V and Λ are guaranteed, ensure a unique value for G_d that leads to (45) for all $0 < \omega < \omega_b$. The detailed proof is not given here because it is lengthy although straightforward. $G_{cl}(j\omega)$ can be expanded in diadic form [11] to show the contribution of the dominant modes (presented by Λ) and the modes of the actuators of the closed-loop system. It can be shown that as ρ approaches ∞ the terms resulting from the actuator modes approach zero while the remaining terms approach $G_r(j\omega)$.

2) *Computation of G_d* : Theorem 4.2.1 can be used to compute G_d . Since, for fast actuator eigenvalues a unique value for G_d guarantees that limit (45) is true for all $0 < \omega < \omega_b$, limit 45 can be used to compute G_d at some frequency in the bounded interval $(0, \omega_b)$. Assume $\omega = 0$ and all eigenvalues of the actuators are located in the left half complex plane farther than any complex number given by Λ . Then from

³ The impedances that always yield a complete set of right eigenvectors are called simple.

limit (45):

$$J_c G_{cl}(0) = G_t(0) \quad (46)$$

where $G_{cl}(0) = H(-A + BG)^{-1}L_p$ and $G_t(0) = K^{-1}$. K is nonsingular and $L_p = (L + BG_d)$. Substituting for $G_{cl}(0)$ and $G_t(0)$ in (46) results in

$$J_c H(-A + BG)^{-1}L_p = K^{-1}. \quad (47)$$

Assume that $G = [G_1 \ G_2 \ G_3]$, $G_1 = n \times n$, $G_2 = n \times n$, $G_3 = n \times n$. Then G_d can be computed from (47) as follows:

$$G_d = [(G_3 + I_{nn})T_s^{-1}GR(\theta_0) + G_1]J_c^{-1}K^{-1} - (G_3 + I_{nn})T_s^{-1}J_c^T. \quad (48)$$

3) *Summary of the Design Method:* The following four steps can be used to design the feedback and feedforward gains for a given θ_0 .

a) Use (31) to compute the $2n$ closed-loop eigenvector u_i associated with the dominant modes. Use (32) to compute m_i , ($i = 1, 2, \dots, 2n$), which identifies the location of u_i in its allowable sub-space. q_i and λ_i are given by (3). This terminates the construction of the dominant modes.

b) Use (36) to compute the n closed-loop eigenvector u_i associated with the actuators. Use (37) to compute m_i , ($i = 2n + 1, 2n + 2, \dots, 3n$), which identifies the location of u_i in its allowable subspace. This terminates the construction of the nondominant modes.

c) Use (38) to compute the state-feedback gain G . The first $n \times n$ partition of G is the joint-angle feedback-gain while the second and the third $n \times n$ partitions of G are the velocity and torque feedback-gains.

d) Use (48) to compute the force-feedforward gain.

4) *Selection of the J -Matrix:* If the conditions of the theorem are satisfied, a unique value for G_d can be found such that limit (45) is true for all $0 < \omega < \omega_b$. In proving Theorem III-B-1, one can show that selection of the J -matrix according to

$$J = J_c^{-T}M(\theta_0)J_c^{-1} \quad (49)$$

will result in $G_d = 0$. This simply means that if the target inertia J is chosen according to (49), then no force measurement is needed to achieve the target dynamics of the theorem. This result is significant, since force measurements are not available for many commercial manipulators. The force measurement can be eliminated if the desired frequency range of operation ω_0 is small enough that it can be parameterized by choosing J according to (49). We do not prescribe a unique value for the J -matrix to parameterize ω_0 . In fact, there exist an infinite number of matrices that can be selected for J to parameterize ω_0 . The size of J is important, not its structure. (One can consider the size of the J -matrix in terms of its singular values.) Here, we summarize some options for the J -matrix. One method is given in Part I of this paper by considering $J = \gamma_1 K$. A designer can also choose the J -matrix to be γI_{nn} , where γ is a positive scalar. Equation (49) motivates us to use (50) to select matrix J . Thus

$$J = \gamma J_c^{-T}M(\theta_0)J_c^{-1} \quad (50)$$

where γ is a positive scalar. Choosing J according to (50) has the advantage of consistency with the natural behavior of the manipulator because $J_c^{-T}M(\theta_0)J_c^{-1}$ is the manipulator inertia matrix in the global coordinate frame. γ in (50) scales the natural inertia of the manipulator equally in all directions. Note that when γ is not unity in equation (50), G_d will not be zero.

C. Stability Robustness and the Eigenstructure of the Actuators

In this section we arrive at a design parameter for stability robustness. Given a nominal model, $G_p(j\omega)$, in (15), an error function $E(j\omega)$ is given according to (16) to represent the uncertainties in the system. If the state-feedback gain G is used to stabilize the nominal model $G_p(j\omega)$, then the real model $G'_p(j\omega)$ will also be stable if inequality (51) is satisfied:

$$\sigma_{\min}[G_0(j\omega)] > e(\omega) \text{ for all } 0 < \omega < \infty \quad (51)$$

where

$$G_0(j\omega) = I_{nn} + [G(j\omega I_{3n3n} - A)^{-1}B]^{-1}$$

and $e(\omega) \geq \sigma_{\min}[E(j\omega)]$. References [18] and [14] leisurely explain this concept in greater depth. The objective is to design G so that inequality (51) is satisfied. The closed-loop eigenstructure of the n actuators is the only freedom left in the design of G . The theorem of Section III-B-1 states that if all the closed-loop eigenvalues of the actuators approach $-\infty$, then the target dynamics represented by (1) can be achieved for all $0 < \omega < \omega_b$. Placement of the closed-loop actuator eigenvalues deep in the left complex plane is not trivial. A trade-off must occur between performance through a wide frequency range and stability robustness.

Suppose the closed-loop eigenvalues of the actuators are located at $\alpha\lambda_{a1}$, $\alpha\lambda_{a2}$, \dots , $\alpha\lambda_{an}$. Scaling all closed-loop actuator eigenvalues to one number preserves bandwidth ratios for the actuators that are consistent with the hardware. Fig. 3 shows that the farther from the origin the n closed-loop eigenvalues of the actuators are located, the larger will be $G(j\omega I_{3n3n} - A)^{-1}B$. Large values for these eigenvalues shift $G(j\omega I_{3n3n} - A)^{-1}B$ up. This is true only when the closed-loop actuator eigenvalues are located much farther from the origin than any complex number offered by A . Since closed-loop actuator eigenvalues that are far from the origin result in a large $G(j\omega I_{3n3n} - A)^{-1}B$ for a wide frequency range, inequality (51) may not be satisfied for all $0 < \omega < \infty$. This is true because a large $G(j\omega I_{3n3n} - A)^{-1}B$ for a wide frequency range allows $G_0(j\omega)$ to remain very close to unity for a wide frequency range, which may, in turn, cause a violation of inequality (51) if $e(\omega)$ does not also remain close to unity for a wide frequency range. On the other hand, according to the theorem in Section III-B-1, the larger α is selected to be, the closer $J_c G_{cl}(j\omega)$ will be to $G_t(j\omega)$ for all $0 < \omega < \omega_b$. So the closed-loop actuator eigenvalues must be placed in the left half complex plane as far as possible without violating the stability robustness specification. In selecting α , $G_0(j\omega)$ must preserve stability robustness specifications at all frequencies. We do not offer any value for α ; it is the designer's choice. Selecting a good value for α requires

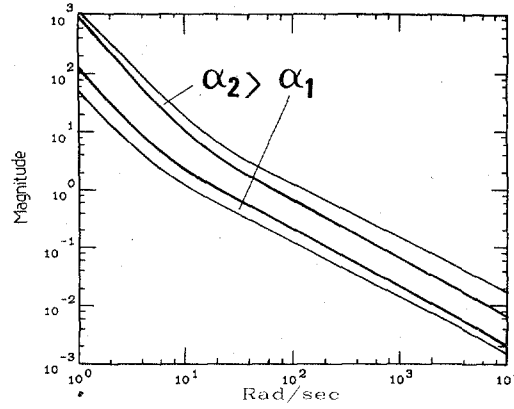


Fig. 3. σ_{\max} and σ_{\min} of $G(j\omega I_{3n3n} - A)^{-1}B$ for various actuator closed-loop eigenvalues.

experience and an understanding of the system. α must be large enough to guarantee that the performance specifications will be met, but small enough to guarantee that the stability robustness specifications will also be fulfilled. The theorem of Section III-B-1 clarifies how a large α can guarantee the performance specifications for a bounded frequency range.

The parameter in the set of performance specifications that can be altered most effectively to meet the stability robustness specifications is ω_0 , the frequency range in which the relationship between interaction force and displacement is approximately independent of frequency. $\delta D(j\omega) \approx K\delta Y(j\omega)$. Shaping the loop transfer function $G(j\omega I_{3n3n} - A)^{-1}B$, for all $0 < \omega < \omega_0$, is the requirement to produce this frequency-independent relationship. On the other hand, one cannot shape $G(j\omega I_{3n3n} - A)^{-1}B$ arbitrarily for an arbitrary frequency range because inequality (51) must be satisfied for all $0 < \omega < \infty$. Satisfying inequality (51) at low frequencies is trivial because of the small size of $e(\omega)$. At larger frequencies, $G(j\omega I_{3n3n} - A)^{-1}B$ must become small to satisfy inequality (51). Therefore, the smaller ω_0 is selected to be, the more robustness to high-frequency unmodeled dynamics can be achieved. Since ω_0 is parameterized by J , it is necessary to consider a larger J (and consequently a smaller ω_0) as a compromise to meet the stability robustness specifications at high frequencies. Of course, the K -matrix can also be altered to change ω_0 . The following summarizes the effects of ω_0 and α on stability robustness.

Increasing ω_0 or α	→	More stability robustness in uncertainties of the modeled dynamics	→	Less stability robustness in high-frequency unmodeled dynamics
Decreasing ω_0 or α	→	Less stability robustness in uncertainties of the modeled dynamics	→	More stability robustness in high-frequency unmodeled dynamics

IV. EXAMPLE AND EXPERIMENT

A. Example

Consider the planar manipulator with two degrees of freedom shown in Fig. 4. Both of its joint angles are powered from the stationary base. The second link is driven by an

actuator on the base via a relatively stiff chain. The mass, length and moment of inertia of each link are represented by δm_i , δx_i , and i_i . The variables i_1 and i_2 are the moments of inertia of the links relative to their end-points. δl_2 locates the center of mass of the second link. The inertia and Jacobian matrices are

$$M(\theta_0) = \begin{pmatrix} i_1 + \delta m_2 \delta x_1^2 & \delta m_2 \delta x_1 \delta l_2 \cos(\theta_2 - \theta_1) \\ \delta m_2 \delta x_1 \delta l_2 \cos(\theta_2 - \theta_1) & i_2 \end{pmatrix}$$

$$J_c = \begin{pmatrix} -\delta x_1 \sin(\theta_1) & -\delta x_2 \sin(\theta_2) \\ \delta x_1 \cos(\theta_1) & \delta x_2 \cos(\theta_2) \end{pmatrix}.$$

Substituting the numerical values for each variable in the inertia matrix and the Jacobian matrix gives

$$M(\theta_0) = \begin{pmatrix} 2.72E-02 & 7.7E-03 \\ 7.7E-03 & 7.44E-03 \end{pmatrix}$$

$$J_c = \begin{pmatrix} -5.05E-01 & -6.48E-1 \\ 8.66E-1 & 6.48E-1 \end{pmatrix}.$$

Since the manipulator is mounted horizontally, gravity does not affect it. The actuator driving θ_1 has a bandwidth of 8 rad/s, while the other actuator has a bandwidth of 10 rad/s. The actuator dynamics can be expressed by matrices A_a and B_a according to (11). Since θ_2 is not the relative angle between the two links and since the actuators are powering the system from a stationary base, $T_s = I_{nn}$ in (8)

$$A_a = \begin{pmatrix} -8 & 0 \\ 0 & -10 \end{pmatrix} \quad B_a = \begin{pmatrix} 8 & 0 \\ 0 & 10 \end{pmatrix}.$$

A , B , and H in (13) and (14) can be written as

$$A = \begin{pmatrix} 0 & 0 & 1 & 0 & 0 & 0 \\ 0 & 0 & 0 & 1 & 0 & 0 \\ 0 & 0 & 0 & 0 & 5.19E+1 & -5.38E+1 \\ 0 & 0 & 0 & 0 & -5.38E+1 & 1.9E+2 \\ 0 & 0 & 0 & 0 & -8 & 0 \\ 0 & 0 & 0 & 0 & 0 & -10 \end{pmatrix}$$

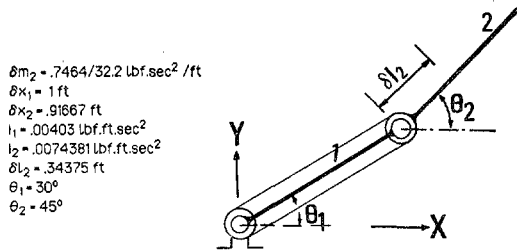


Fig. 4. Manipulator with two degrees-of-freedom.

$$B = \begin{pmatrix} 0 & 0 \\ 0 & 0 \\ 0 & 0 \\ 0 & 0 \\ 8 & 0 \\ 0 & 10 \end{pmatrix}, \quad H = \begin{pmatrix} 0 & 0 \\ 0 & 0 \\ 8.87 & 10.15 \\ -96.32 & -10.14 \\ 0 & 0 \\ 0 & 0 \end{pmatrix}$$

$$H = \begin{pmatrix} 1 & 0 & 0 & 0 & 0 & 0 \\ 0 & 1 & 0 & 0 & 0 & 0 \end{pmatrix}$$

The designer must provide not only the nominal model for the manipulator but also the bound for the uncertainties $e(\omega)$. The model uncertainty for this example is given by $e(\omega)$ in Fig. 1. $e(\omega)$ takes the value of 0.4 at low frequencies and rises to 2 at 35 Hz. The first unmodeled mode that represents a bending dynamic of the manipulator takes place at 35 Hz (220 rad/s) with $e(220) = 2$. The large magnitude of $e(\omega)$ at 220 rad/s shows that the unmodeled mode is under-damped. Most space manipulators have under-damped structural modes. The large values for $e(\omega)$ at high frequencies for under-damped unmodeled modes force designers to design low-bandwidth systems to avoid possible instabilities. According to this model uncertainty, the dynamic model is nearly valid for an approximate range of 10 Hz.

The design specifications in the global cartesian coordinate frame are

- 1) stiffness in the X -direction = 0.615 lbf/ft, for $0 < \omega < 6.283$ rad/s (1 Hz)
- 2) stiffness in the Y -direction = 12.3 lbf/ft, for $0 < \omega < 6.283$ rad/s.

Note that the desired frequency range of operation is selected within the range for which the model is nearly valid. The stiffness ratio is about 20. The low stiffness in the X -direction generates a "soft" positioning system for the end-point along the X -direction, while a larger stiffness in the Y -direction guarantees a relatively "stiff" positioning system in that direction. Note that the natural behavior of the manipulator in the configuration shown in Fig. 4 opposes the desired

performance specification. In other words, the inertia of the manipulator in the global Cartesian frame $J_c^{-T}M(\Theta_0)J_c^{-1}$ makes it much easier to keep the manipulator "softer" in the Y -direction than in the X -direction. The following diagonal target dynamics are proposed to order the design specifications into parameters:

$$K = \begin{pmatrix} .61 & 0 \\ 0 & 12.3 \end{pmatrix}$$

$$C = \begin{pmatrix} 7.99E-2 & 0 \\ 0 & 1.24 \end{pmatrix}$$

$$J = \begin{pmatrix} 2.47E-3 & 0 \\ 0 & 2.97E-2 \end{pmatrix}$$

The diagonal inertia matrix and the diagonal damping matrix are selected such that the stiffness value for each direction guarantees the desired behavior within a frequency range of 6.283 rad/s. Note that since we choose a diagonal target dynamics, selection of J - and C -matrices for a given K -matrix is trivial. We choose each member of C and J such that, at each direction, a slightly over-damped, stable, second-order impedance results. The transfer function of the target dynamics $G_r(s)$ is

$$G_r(s) = \begin{pmatrix} 1.625 \frac{1}{(s/12.62+1)(s/19.72+1)} & 0 \\ 0 & .0812 \frac{1}{(s/16.29+1)(s/25.46+1)} \end{pmatrix}$$

Fig. 5 shows how the equation that expresses the target dynamics of the system, $G_r(s) = (Js^2 + Cs + K)^{-1}$, represents the desired stiffness values and frequency range of operation. The eigenstructure of the target dynamics can be represented by V and Λ :

$$\Lambda = \{-12.62, -19.72, -16.29, -25.46\}$$

$$V = \begin{pmatrix} 2.73 & 2.73 & 2.73 & 2.73 \\ -3.65 & -3.65 & -2.11 & -2.11 \\ -34.48 & -53.88 & -44.51 & -69.55 \\ 46.07 & 71.98 & 34.34 & 53.65 \end{pmatrix}$$

For $\alpha = 5$, the closed-loop eigenvalues of the actuators are located at -40 and -50 . This preserves the bandwidth ratio of 8/10 for the actuators. The set of closed-loop eigenvalues S is given by $S = \{-12.62, -19.72, -16.29, -25.46, -40., -50.\}$. Using (31) and (36), U can be computed to be

$$U = \begin{pmatrix} 2.73 & 2.73 & 2.73 & 2.73 & 3.25E-2 & -2.15E-2 \\ -3.65 & -3.65 & -2.10 & -2.11 & -3.26E-2 & 7.6E-2 \\ -34.48 & -53.88 & -44.51 & -69.55 & -1.30 & 1.07 \\ 46.07 & 71.98 & 34.34 & 53.65 & 1.34 & -3.80 \\ 7.37 & 17.98 & 15.43 & 37.67 & 1 & 0 \\ -0.97 & -2.38 & 1.42 & 3.47 & 0 & 1 \end{pmatrix}$$

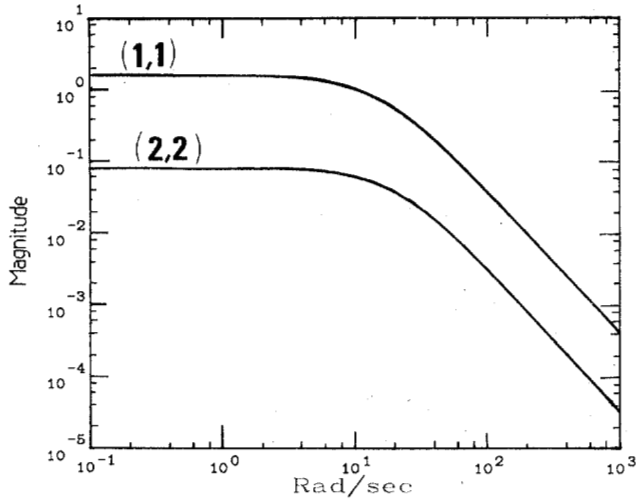


Fig. 5. Target dynamics $G_c(j\omega)$. The numbers in the parenthesis indicate the row and column of each member of the matrix, respectively.

Note that the first 4×4 members of U are identical to V . Equations (32) and (37) can be used to compute $m_i (i = 1, 2, \dots, 6)$ as follows:

$$\begin{pmatrix} -4.25 & -26.35 & -15.99 & -82.20 & -4 & 0 \\ 0.25 & 2.31 & -0.89 & -5.36 & 0 & -4 \end{pmatrix}.$$

The state-feedback gain G and force-feedforward gain can be computed via (38) and (48). Thus

$$G = \begin{pmatrix} 70.23 & 36.21 & 8.08 & 3.53 & 8.69 & 3.49 \\ 13.94 & 12.45 & 1.78 & 1.63 & 0.08 & 7.66 \end{pmatrix}$$

$$G_d = \begin{pmatrix} 104.09 & -1.27 \\ -6.31 & -4.72 \end{pmatrix}$$

The size of α is limited by the stability of robustness specifications. Fig. 6 shows that large values for α will lead to a violation of the stability robustness specifications of (51) for $\alpha = 10$ and meets the stability robustness specifications for $\alpha = 5$. Large values of α result in large G , which leads to large values of $G(sI_{3n3n} - A)^{-1}B$. Fig. 7 shows the closed-loop transfer function $J_c G_{cl}(s)$ for various values of α . The larger α is selected to be, the closer the closed-loop transfer function $J_c G_{cl}(s)$ will be to $G_t(s)$ for a bounded frequency range. For small values of α , the members of $J_c G_{cl}(s)$ will exhibit strong coupling; therefore, satisfaction of the performance specifications is not guaranteed at low frequencies. On the other hand, large values of α result in a trivial coupling between the members of $J_c G_{cl}(s)$ at low frequencies (as long as $G_0(j\omega) = I_{3n3n} + [G(j\omega I_{3n3n} - A)^{-1}B]^{-1}$ does not violate the stability robustness specifications). Even though a large α ensures better performance, it produces large values for the state-feedback gain G and the force-feedforward gain G_d . The transfer function matrix $J_c G_{cl}(j\omega)$ is as follows for $\alpha = 5$:

$$\begin{pmatrix} 1.62 \frac{(s/310 + 1)(s/46 + 1)}{(s/12.62 + 1)(s/19.72 + 1)} \\ -4.28E-3 \frac{s(s/65.8 + 1)}{(s/16.29 + 1)(s/25.46 + 1)} \end{pmatrix}$$

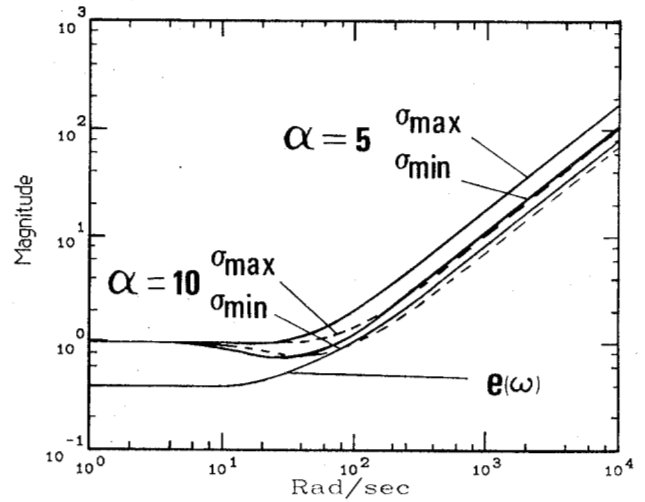


Fig. 6. σ_{max} and σ_{min} of $G_0(j\omega)$ for $\alpha = 5$ and $\alpha = 10$.

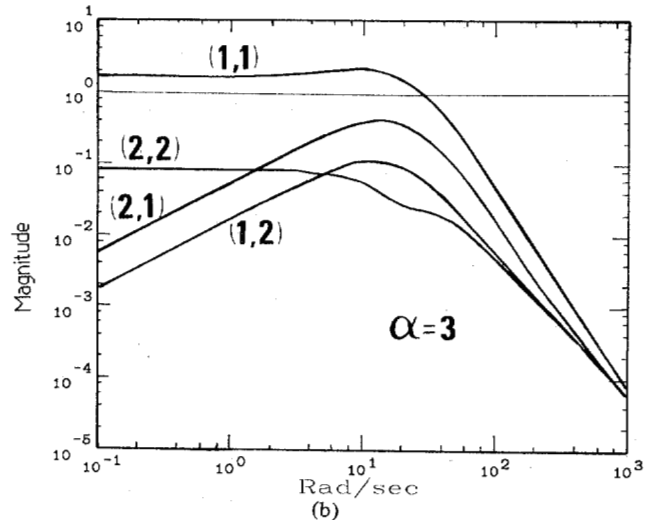
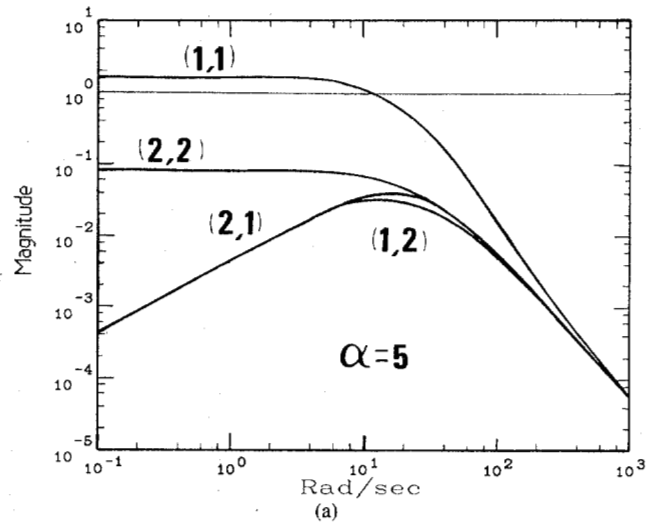


Fig. 7. Closed-loop transfer function matrix $J_c G_{cl}(j\omega)$.

$$\begin{pmatrix} -4.42E-3 \frac{s(s/41 + 1)}{(s/12.62 + 1)(s/19.72 + 1)} \\ 0.0812 \frac{(s/32 + 1)(s/37 + 1)}{(s/16.29 + 1)(s/25.4 + 1)} \end{pmatrix}$$

The off-diagonal members of $J_c G_{cl}(j\omega)$ for $\alpha = 5$ are much smaller than the diagonal members and therefore, the plot of $J_c G_{cl}(j\omega)$ in Fig. 7 resembles the target dynamics in Fig. 5, for all $0 < \omega < \omega_0$.

B. Experiment

A simple experiment is described here to show how impedance control can be employed to develop compliancy on a planar positioning table. This experiment also points out the difference between employment of impedance control and admittance control in constrained maneuver. The positioning table consists of a platform driven by two DC motors via two lead-screw mechanisms (Fig. 8). The goal of the overall project is to develop a positioning system with different stiffnesses and different bandwidths along the two axes of a global cartesian coordinate frame by an on-line computer. The axes of this global coordinate frame do not necessarily coincide with the axes of the motors. In this section, we are interested in observing the transient behavior of the table from unconstrained maneuvers to constrained maneuvers when (1) is guaranteed for the system. To show this transient behavior, we describe the result of an experiment when only one axis is employed (one dimension case). Fig. 8 shows this simple set-up. A wide bandwidth force sensor is mounted on the platform to measure the contact force along two orthogonal directions [6].

A computer algorithm with 0.01-s sampling time was designed and implemented on a microcomputer to develop compliancy on the table as in (1). The controller is able to accept the stiffness, bandwidth and damping coefficient (three items of the set of performance specifications given in Part one in addition to the set-point position-command). The platform was commanded to move beyond a solid surface. Fig. 9(b) is the periodic ramp position command generated by the computer to the system. Fig. 9(a) is the contact force. For this experiment, K is chosen to be 3.5 lbf/in while the bandwidth of the system is 4 Hz. As long as the force sensor is not in touch with the stiff wall, the contact force is zero. After the force sensor touches the stiff wall, the contact force increases proportionally to the commanded input position [$\delta D(t) \approx K\delta Y(t)$]. Since the input position command is a ramp function, the contact force is also a ramp function.

Note that we have a positioning system for the table that has the ability to modulate the impedance of the system. In other words, it accepts a set-point position, and it reflects a force as output. We do not command any set-point force as we do in admittance control. By assigning various position commands and by maintaining complete control on (1), we can keep the contact force in a desired range.

CONCLUSION

The target impedance mandates a closed-loop relationship between the interaction loads and the motion of the system in the global cartesian coordinate frame. In general, the closed-loop behavior of a system cannot be shaped arbitrarily over an arbitrary, bounded frequency range. However, we show that this target impedance is mathematically achievable, and in Section III we offer a geometrical design method to achieve it.

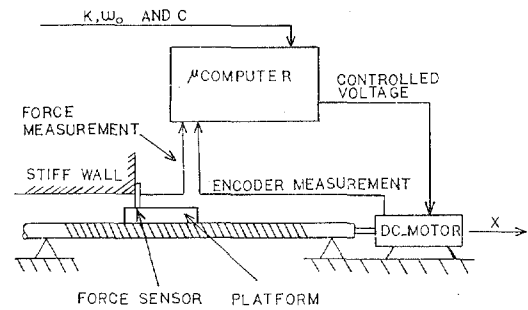


Fig. 8. Planar positioning table.

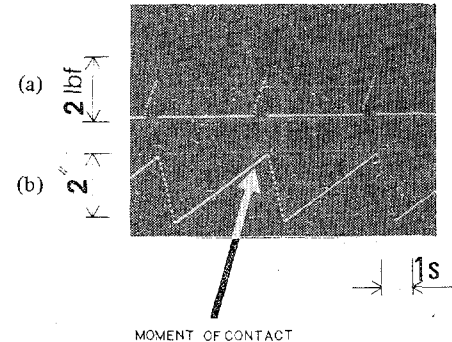


Fig. 9. (a) Contact force. (b) Commanded position.

By considering the dynamics of the manipulators and its actuators, continuous feedback and feedforward gains are given in closed form to guarantee the achievement of the target dynamics in the presence of model uncertainties.

To achieve the target impedance given by (1), we need to measure the joint angles, joint angle rates, actuator torques, and interaction forces of the system. Most direct-drive manipulators are not equipped with fast actuators, and it is necessary to consider their dynamics and to measure the actuator torques (or motor currents) in the design process if a wide frequency range of operation is needed. In Section II we develop a mathematical model for manipulators and their actuators to represent their dynamic behavior during low-speed constrained maneuvers. When the actuators are fast (i.e., their bandwidths are much wider than the desired frequency range of operation ω_0), the dynamics of the actuators can be neglected, which eliminates the need for torque feedback. If ω_0 is small enough to be parameterized by the target inertia matrix given by (49), then force measurement can also be eliminated. In other words, if the target inertia is selected to be the inertia of the manipulator in the global coordinate frame, given by (49), then it is not necessary to measure the interaction forces. We use force-feedforward only to change the inertia of the system. If the actuators are fast and the frequency range of operation is small enough that the target inertia can be chosen according to (49), then it is necessary to measure only the joint angles and joint angle rates.

Stability in the presence of model uncertainties is another significant issue in our design method. Large feedback gains produce poor robustness to high-frequency unmodeled dynamics and good robustness to uncertainties within the modeled dynamics. Selecting a wide ω_0 will produce a large

feedback gain, which means the system will be less robust to high-frequency unmodeled dynamics and more robust to uncertainties in the modeled dynamics. On the other hand, a narrow ω_0 will result in a small state-feedback gain, which will assure good robustness to high-frequency unmodeled dynamics. Since ω_0 is parameterized by J , we can state that for a given K , a small J -matrix may cause instability in the presence of high-frequency unmodeled dynamics, and a large J -matrix may cause instability if there are uncertainties in the model at low frequencies.

The trade-off between the size of the target inertia and stability robustness relative to high-frequency unmodeled dynamics is another contribution of this paper. Another factor in the size of the state-feedback gain is α , which measures the locations of the closed-loop eigenvalues of the actuators. The farther from the origin the n closed-loop eigenvalues of the actuators are located, the larger the feedback gain matrix G will be. In other words, wide closed-loop bandwidths of actuators result in less robustness to high frequency unmodeled dynamics.

REFERENCES

- [1] J. C. Doyle and G. Stein, "Multivariable feedback design: concepts for a classical/modern synthesis," *IEEE Trans. Auto. Contr.*, vol. AC-26, no. 1, pp. 1-16, Feb. 1981.
- [2] M. M. Fahmy and J. O'Reilly, "On eigenstructure assignment in linear multivariable systems," *IEEE Trans. Auto. Contr.*, vol. AC-27, no. 3, pp. 690-693, June 1982.
- [3] ———, "Eigenstructure assignment in linear multivariable systems—A parametric solution," *IEEE Trans. Auto. Contr.*, vol. AC-28, no. 10, pp. 990-994, Oct. 1983.
- [4] F. R. Gantmacher, *The Theory of Matrices*. New York: Chelsea, 1977.
- [5] I. Gohberg, L. Lancaster, and L. Rodman, *Matrix Polynomials*. New York: Academic, 1982.
- [6] R. L. Gott, "An approach to automated deburring using an industrial robot," M.S. thesis, Mechanical Engineering Department, M.I.T., Cambridge, MA, July 1985.
- [7] C. A. Harvey and G. Stein, "Quadratic weights for asymptotic regular properties," *IEEE Trans. Auto. Contr.*, vol. AC-23, no. 3, pp. 378-387, June, 1978.
- [8] J. M. Hollerbach, "A recursive Lagrangian formulation of manipulator dynamics and a comparative study of dynamics formulation complexity," *IEEE Trans. Syst., Man, Cybern.*, vol. SMC-10, no. 11, pp. 730-736, Nov. 1980.
- [9] ———, "Dynamic Scaling of Manipulator Trajectories," *ASME J. Dynamic Syst., Measurement, Contr.*, vol. 106, pp. 102-106, Mar. 1984.
- [10] K. Huseyin, *Vibrations and Stability of Multiple Parameter Systems*. Amsterdam: Sijthoff and Noordhoff, 1978.
- [11] T. Kailath, *Linear Systems*. Englewood Cliffs, NJ: Prentice-Hall, 1980.
- [12] G. Klein and B. C. Moore, "Eigenvalue-generalized eigenvector assignment with state-feedback," *IEEE Trans. Auto. Contr.*, vol. AC-22, no. 1, pp. 140-141, Feb. 1977.
- [13] P. Lancaster, *Lambda-Matrices and Vibrating Systems*. New York: Pergamon, 1966.
- [14] N. A. Lehtomaki, N. R. Sandell, and M. Athans, "Robustness results in linear-quadratic Gaussian-based multivariable control designs," *IEEE Trans. Auto. Contr.*, vol. AC-26, no. 1, pp. 75-92, Feb. 1981.
- [15] B. C. Moore, "On the flexibility offered by state-feedback in multivariable systems beyond closed-loop eigenvalue assignment," *IEEE Trans. Auto. Contr.*, vol. AC-21, no. 5, pp. 689-692, Oct. 1976.
- [16] B. Porter and J. J. D'azzo, "Closed-loop eigenstructure assignment by state-feedback in multivariable linear systems," *Int. J. Contr.*, vol. 27, no. 3, pp. 487-492, 1978.
- [17] ———, "Algorithm for closed-loop eigenstructure assignment by state-feedback in multivariable linear systems," *Int. J. Contr.*, vol. 27, no. 6, pp. 943-947, 1978.
- [18] M. G. Safonov and M. Athans, "Gain and phase margin for multiloop LQG regulators," *IEEE Trans. Auto. Contr.*, vol. AC-22, no. 2, pp. 173-179, Apr. 1977.
- [19] W. M. Silver, "On the equivalence of Lagrangian and Newton-Euler dynamics for manipulators," *Int. J. Robotics Res.*, vol. 1, no. 2, pp. 60-70, 1982.
- [20] G. Strang, *Linear Algebra and Its Applications*. New York: Academic, 1976.
- [21] "Speed controls, servo systems. An engineering handbook," Electro-Craft Corp., Hopkins, MN.

H. Kazerooni, for a photograph and biography see p. 92 of the June 1986 issue of this TRANSACTIONS.

Paul K. Houpt (S'73-M'75), for a photograph and biography see p. 92 of the June 1986 issue of this TRANSACTIONS.

Thomas B. Sheridan (M'60-SM'82-F'80), for a photograph and biography see p. 92 of the June 1986 issue of this TRANSACTIONS.